

Low Dielectric Polyimide Aerogels As Substrates for Lightweight Patch Antennas

Mary Ann B. Meador,^{*,†} Sarah Wright,^{†,‡} Anna Sandberg,^{†,‡} Baochau N. Nguyen,[§] Frederick W. Van Keuls,[⊥] Carl H. Mueller,[#] Rafael Rodríguez-Solís,^{||} and Félix A. Miranda[†]

[†]NASA Glenn Research Center, 21000 Brookpark Road, Cleveland, Ohio 44135, United States

[§]Ohio Aerospace Institute, 22800 Cedar Point Road, Cleveland, Ohio 44135, United States

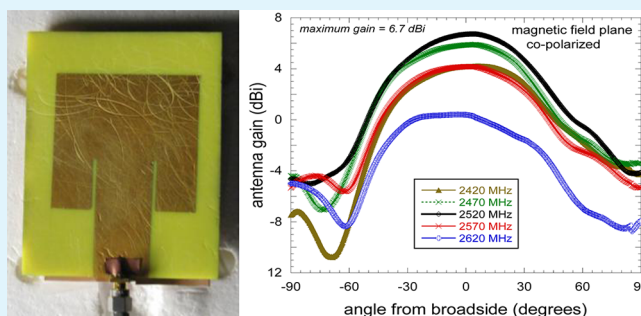
[⊥]Vantage Partners, LLC, 3000 Aerospace Parkway, Brook Park, Ohio 44142, United States

[#]Qinetiq North America, 1100 Apollo Drive, Brook Park, Ohio 44142, United States

^{||}University of Puerto Rico-Mayagüez, Mayagüez, Puerto Rico

ABSTRACT: The dielectric properties and loss tangents of low-density polyimide aerogels have been characterized at various frequencies. Relative dielectric constants as low as 1.16 were measured for polyimide aerogels made from 2,2'-dimethylbenzidine (DMBZ) and biphenyl 3,3',4,4'-tetracarboxylic dianhydride (BPDA) cross-linked with 1,3,5-triaminophenoxybenzene (TAB). This formulation was used as the substrate to fabricate and test prototype microstrip patch antennas and benchmark against state of practice commercial antenna substrates. The polyimide aerogel antennas exhibited broader bandwidth, higher gain, and lower mass than the antennas made using commercial substrates. These are very encouraging results, which support the potential advantages of the polyimide aerogel-based antennas for aerospace applications.

KEYWORDS: aerogels, polyimides, low dielectric, antennas, mesoporous



INTRODUCTION

Depending on the ability to overcome poor mechanical properties or environmental stability, low-density aerogels have many potential applications, including thermal and electrical insulation, catalyst supports, and filtration.¹ We have explored the use of low thermal conductivity, durable aerogels, including polymer-reinforced silica aerogels² and more recently polyimide aerogels,^{3–5} as thermal insulation for a number of demanding aerospace applications including inflatable aerodynamic decelerators for planetary entry, descent, and landing operations.⁶

In addition to low thermal conductivity and density, aerogels possess very low dielectric properties. For example, Hrubesh et al. characterized the dielectric constants and loss tangent components of the complex relative permittivity for a series of silica and melamine formaldehyde aerogels at high frequencies.⁷ It was found that dielectric constants varied linearly with density for both silica and organic aerogels. Dielectric constants as low as 1.008 were measured for silica aerogels with densities as low as 0.008 g/cm³. On the other hand, loss tangents that also tracked density were shown to be affected by water absorbed on the large internal surface areas of the aerogels.

This sensitivity to moisture in addition to the fragility of the aerogels makes it difficult to take advantage of the low dielectric properties for practical applications, such as antennas. If these difficulties are overcome, lightweight antennas made from low

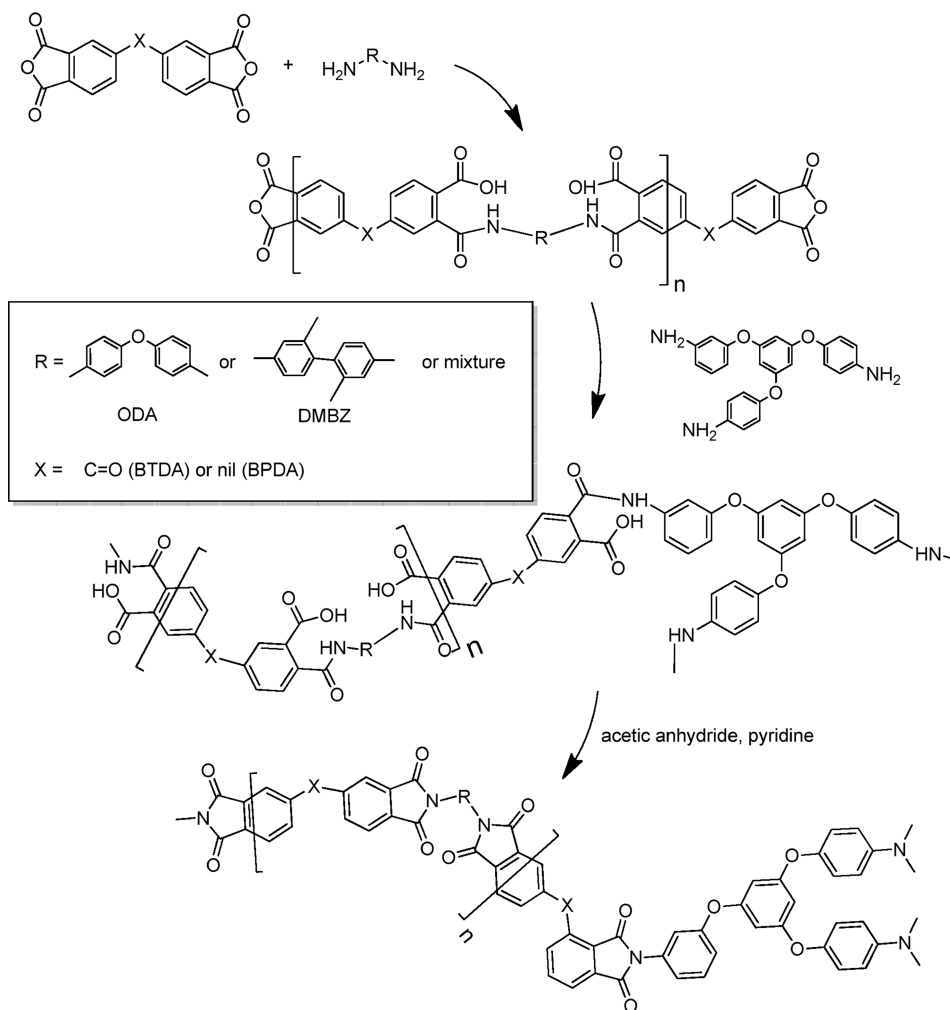
density and low dielectric permittivity aerogels could exhibit reduced radio frequency (RF) losses and improved impedance matching, as well as higher gain, larger bandwidth, and lower mass than current state of practice (SOP) counterparts.⁸ The design and optimization of communication system technologies in support of aerospace platforms is of paramount interest in the aviation industry, for government and the commercial sector. Among the key technologies are transmit/receive (Tx/Rx) antennas required for communications (voice, high data rate video, Internet, etc.) and navigation (GPS).^{9,10} A typical commercial and/or military aircraft (e.g., Boeing 737) could have as many as 15 to 100 antenna systems. This large number of antennas not only adds weight to the aircraft but also increases the complexity, and challenges the structural integrity of the fuselage. The latter is exacerbated in commuter and general aviation aircraft because of more limited space for antenna placement. Therefore, approaches that could reduce the mass and number of antennas in aircraft and any other pertinent airborne platform (e.g., long duration, high altitude elevation platforms) without sacrificing performance are highly desired.^{11,12}

Received: September 13, 2012

Accepted: October 25, 2012

Published: November 7, 2012

Scheme 1. Synthesis of Polyimide Aerogels with TAB Cross-Links



Low dielectric properties have also been reported for porous polyimides fabricated through, for example, extraction of porogens from precursor films,¹³ use of mesoporous nanoparticle fillers in the films,¹⁴ and vapor induced phase separation at high temperatures.¹⁵ The latter produced the lowest dielectric constants (1.67) for polyimide films with densities less than 0.4 g/cm^3 . We have recently reported the fabrication of porous polyimide aerogels by cross-linking anhydride capped oligomers with 1,3,5-tris(aminophenoxy)benzene, TAB, followed by chemical imidization at room temperature, and supercritical liquid CO_2 extraction.⁴ The aerogels had densities as low as 0.13 g/cm^3 , depending on the oligomers used. The aerogels can be fabricated as thick parts with compressive modulus of 20 MPa, and stand-alone flexible films with tensile strength as high as 8.7 MPa. These mechanical properties combined with sufficiently low dielectric properties may enable new antenna concepts with performance characteristics (wide bandwidth and high gain) and material properties (low density, environmental stability, and robustness) superior to the state of practice.

In this paper, a series of polyimide aerogels using TAB as the cross-linker are fabricated to characterize electromagnetic properties such as permittivity ($\epsilon_r = \epsilon_r' + j\epsilon_r''$), and loss tangent ($\tan \delta = \epsilon_r''/\epsilon_r'$), where ϵ_r' is known as the relative dielectric constant of the material with respect to the permittivity of vacuum ($\epsilon_0 = 8.85 \times 10^{-12} \text{ F/m}$) and $\tan \delta$ is associated with

the propagation losses of the material at RF frequencies. Previous studies^{4,5} show that different backbone chemistry leads to differing amounts of shrinkage of the polyimide aerogels during processing and hence different densities. Because dielectric properties of silica aerogels vary linearly with density, it is of interest to examine the effect of density on dielectric properties of the polyimide aerogels. Hence, two different dianhydrides and two diamines are used in fabricating the aerogels, and their effect on electromagnetic and other properties is examined. A prototype microstrip patch antenna from the aerogel formulation with the lowest dielectric constant and lowest loss tangent is also fabricated and benchmarked against current antenna technology.

EXPERIMENTAL SECTION

Materials. 1, 3, 5-Triaminophenoxybenzene (TAB) was obtained from Triton Systems (200 Turnpike Rd # 2, Chelmsford, MA 01824-4053). Pyridine, acetic anhydride, and anhydrous N-methylpyrrolidone (NMP) were purchased from Sigma Aldrich. 2,2'-Dimethylbenzidine (DMBZ), 4,4'-oxydianiline (ODA), benzophenone-3,3',4,4'-tetracarboxylic dianhydride (BTDA), and biphenyl-3,3',4,4'-tetracarboxylic dianhydride (BPDA) were obtained from Chriskev, Inc. (13920 W 108th Street, Lenexa, Kansas, 66215). Dianhydrides were dried at $125 \text{ }^\circ\text{C}$ in vacuum for 24 h before use. All other reagents were used without further purification.

Table 1. Properties of Polyimide Aerogels in the Study^a

sample	dianhydride	diamine (% DMBZ)	density, (g/cm ³)	modulus (MPa)	dielectric constant, X-band	loss tangent, X-band	dielectric constant, low freq.	loss tangent, low freq.	dielectric constant, Ka-band	loss tangent, Ka-Band
1	BPDA	0	0.207	13.9	1.266	8.74×10^{-3}				
2	BPDA	0	0.163		1.2230	7.00×10^{-3}			1.227	7.00×10^{-3}
3	BPDA	0.25	0.130	16.0	1.1700	4.70×10^{-3}			1.185	4.71×10^{-3}
4	BPDA	0.75	0.159	43.7	1.158	4.33×10^{-3}	1.260	6.77×10^{-3}		
5	BPDA	0.75	0.108		1.136	5.68×10^{-3}			1.133	1.78×10^{-3}
6	BPDA	0.50	0.188	33.9					1.214	3.37×10^{-3}
7	BPDA	0.50	0.195	28.1						
8	BPDA	1.00	0.111	19.1	1.155	3.90×10^{-3}			1.145	1.57×10^{-3}
9	BPDA	1.00	0.131	20.1	1.159	1.10×10^{-3}	1.249	1.54×10^{-3}		
10	BTDA	0	0.264	6.7						
11	BTDA	0.25	0.195	17.8	1.246	4.69×10^{-3}				
12	BTDA	0.50	0.196		1.249	4.13×10^{-3}				
13	BTDA	1.00	0.210	102.3	1.280	4.13×10^{-3}			1.289	2.68×10^{-3}
14	BTDA	0.75	0.197	56.2	1.239	4.60×10^{-3}	1.356	1.04×10^{-3}		
15	BTDA	0.50	0.203	18.6	1.268	6.02×10^{-3}	1.320	1.13×10^{-3}	1.320	1.30×10^{-3}
16	BTDA	1.00	0.195	58.4	1.285	5.30×10^{-3}	1.355	4.05×10^{-3}		

^aBlank space indicates that sample run was not measured at these conditions.

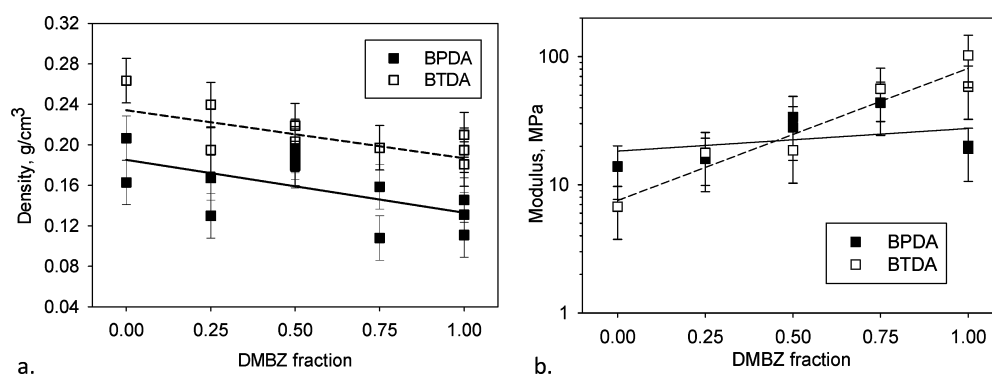


Figure 1. Graphs of (a) density and (b) modulus from compression graphed vs DMBZ fraction for various formulations of aerogels. Error bars represent one standard deviation from empirical modeling of the pooled data.

Rogers Duroid 6010 and Rogers Duroid 5880 laminates were obtained from Rogers Corporation (100 S. Roosevelt Avenue, Chandler, AZ 85226).

Synthesis of Polyimide Aerogels Using Chemical Imidization. Polyimide aerogels were prepared as previously described⁴ and as shown in Scheme 1 using either BPDA or BTDA as the dianhydride formulated with $n = 30$. The diamines used were either ODA or DMBZ or a mixture of the two as shown in Table 1. The table lists the diamine concentration expressed as the % DMBZ used as a percentage of the total diamine (with ODA as 100 – % DMBZ implied).

Permittivity Measurements. The waveguide transmission measurement technique employed for the measurement of the dielectric properties of the aerogel has been previously described.¹⁶ The reliability of this technique has been corroborated by measuring known materials such as magnesium oxide (MgO), zirconium oxide, and sapphire substrates, among others. For low frequency measurements, for which we used the parallel plate capacitor technique, Teflon was used as a control and the obtained values correlate well with that reported in the literature (~ 2.1). Specimen geometries were dictated by the permittivity tests and ranged from approximately $W = 1.5$ cm, $H = 1.5$ cm, and $T = 0.25$ cm for low-frequency measurements (~ 0.050 – 1.3 GHz) using the parallel plate capacitor technique, $W = 2.29$ cm, $H = 1.02$ cm, and $T = 0.74$ cm for the X-Band (~ 11 – 12 GHz) waveguide transmission measurement, and $W = 0.35$ cm, $H = 0.71$ cm, and $T = 0.25$ cm for the Ka-Band (30–40 GHz) waveguide transmission measurement, where W = width of the sample, H = sample height, and T = sample thickness as shown in Figure 5. The

low-frequency measurements were performed using the Agilent model 16453A dielectric material test fixture, whereas the measurements at X- and Ka-Band were performed using Agilent Technologies E8361A performance network analyzer (PNA) with the 85071E material measurements software feature.

Antenna Patterning. For the Rogers Duroid substrates, the antenna pattern was defined in a ruby mask and subsequently transferred to the substrates via a photolithographic process. The photolithography process included spinning photo resist (Shipley 1813) over the substrate, and curing it at 90 °C for 30 min. Afterward, and with the ruby mask in place, the sample was exposed to UV light using a Colight M-129 exposure unit under vacuum conditions for 60 s. After removing the sample from the exposure unit, the sample was placed in a developer solution of deionized water and AZ 352 Developer 3:1 for pattern definition. The sample was subsequently blown dry with nitrogen gas and heated to 110 °C in an oven for 30 min. Finally, the sample was placed in a copper etching tank (VPR-70) for removal of copper from the nonpatterned area on the substrate, and then cleaned with acetone and ethanol to remove any remaining photo resist. The aerogel antenna pattern was applied using e-beam evaporation and a copper shadow mask. For all antennas, the ground plane was deposited with e-beam evaporated gold on the opposite side of the patch.

Compression Tests. The specimens were tested as previously described⁴ in accordance with ASTM D695–10 with the sample sizes nominally 1.5–1.8 cm in diameter and 3 cm in length (close to the 1 to 2 ratio of diameter to length prescribed for the testing of polymer

foams). The samples were tested between a pair of compression platens on a Model 4505 Instron load frame using the Series IX data acquisition software. The platen surfaces were coated with a graphite lubricant to reduce the surface friction and barreling of the specimen. Modulus was taken as the initial slope of the stress strain curve and is reported in Table 1.

RESULTS AND DISCUSSION

Formulations of polyimide aerogels with different backbone chemistry were fabricated according to Scheme 1. Previously,

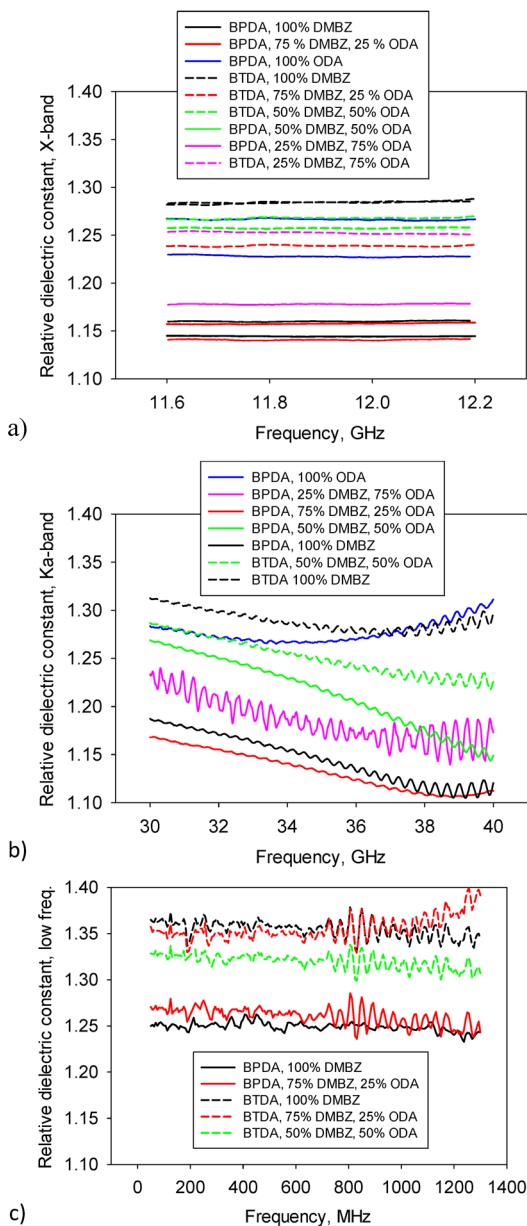


Figure 2. Relative dielectric constants at (a) X-Band, (b) Ka-band, and (c) low frequency for various formulations of aerogels (average of two measurements).

physical and mechanical properties of TAB cross-linked aerogels from two different dianhydrides, BPDA and BTDA, and two diamines, ODA and DMBZ were reported.⁴ It was found that aerogel properties (density, mechanical properties) were highly dependent on the amount of shrinkage occurring during gelation. Aerogels made using a combination of BPDA

and DMBZ shrank the least and therefore had the lowest density, whereas using BTDA and ODA led to greater shrinkage and higher densities. Aerogels made using ODA also tended to be less brittle, whereas DMBZ aerogels tended to decompose at a lower temperature. This was also found to be the case in a related study of polyimide aerogels cross-linked with octa(aminophenyl)polyoligomeric silsesquioxane, OAPS instead of TAB.⁵ Furthermore, it was found that using mixtures of diamines led to improved combinations of properties. For example, whereas 100% ODA gives flexible aerogels that are hydrophilic and DMBZ gives more hydrophobic aerogels that are more brittle, a mixture of 50% ODA and 50% DMBZ used in conjunction with BPDA gives polyimide aerogels with better moisture resistance, and flexibility. Hence, in this study, mixtures of ODA and DMBZ were examined as shown in Table 1. The amount of DMBZ used is shown as a percentage of the total diamine, while the amount of ODA is 100 - DMBZ %.

As seen in Figure 1a, density (standard deviation = 0.015, $R^2 = 0.83$) decreases with increasing DMBZ fraction for aerogels made using BPDA or BTDA, due to the propensity for DMBZ to decrease shrinkage during processing. This shrinkage, which occurs mostly during gelation, may be due to increased rigidity of the polymer chains compared to ODA or less interaction between the gelation solvent (NMP) and the polymer backbone. A graph of modulus from compression vs DMBZ fraction is shown in Figure 1b. Note that although modulus of aerogels usually scales with density, here modulus actually increases with increasing DMBZ fraction, especially when BTDA is the dianhydride. This increase is probably due to increased stiffness of the polymer chains using DMBZ and has been observed previously in similar polyimide aerogels cross-linked using OPAS.⁵

Formulations of the PI aerogels were also fabricated in sizes suitable for dielectric characterization at multiple bandwidths. The polyimide aerogels were fabricated from silicone molds and sanded to exact sizes needed for RF characterization at multiple frequencies. RF characterization was performed to evaluate the relative dielectric constant and loss tangent of the aerogels at operational frequencies of interest for fabrication of antennas.

Relative dielectric constants for several aerogel formulations are shown in Figure 2 at three different frequency ranges. Panels a and b in Figure 2 show dielectric measurements in the microwave region of the electromagnetic spectrum known as the X-band and Ka-band, respectively, whereas Figure 2c shows measurements at low frequencies, i.e., in the submicrowave frequency range. These frequency ranges are representative of ranges typically used for aeronautics and aerospace communications. The values of all relative dielectric constants measured for all frequencies and all formulations fall in the range of 1.1 to 1.4, comparable to silica aerogels of similar density. Significantly, the low dielectric constants enable the development of microstrip patch antennas with better impedance matching and higher gain than equivalent versions fabricated in conventional substrates with higher dielectric constants. Note that a slight decrease in the value of the dielectric constant with increasing frequency is observed. Typically, a decreasing dielectric constant with frequency is expected as the contribution from the dipolar polarizability drops with frequency in the microwave region.¹⁷

In general, it is observed that relative dielectric constant is lower for aerogels made using BPDA as the dianhydride

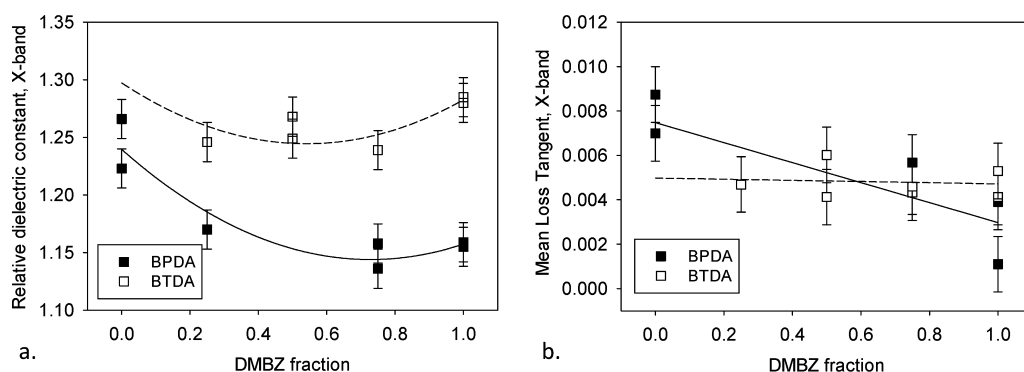


Figure 3. Graphs of (a) relative dielectric constant and (b) loss tangent from X-band measurements graphed vs DMBZ fraction for various formulations of aerogels. Error bars represent one standard deviation from empirical modeling of the pooled data.

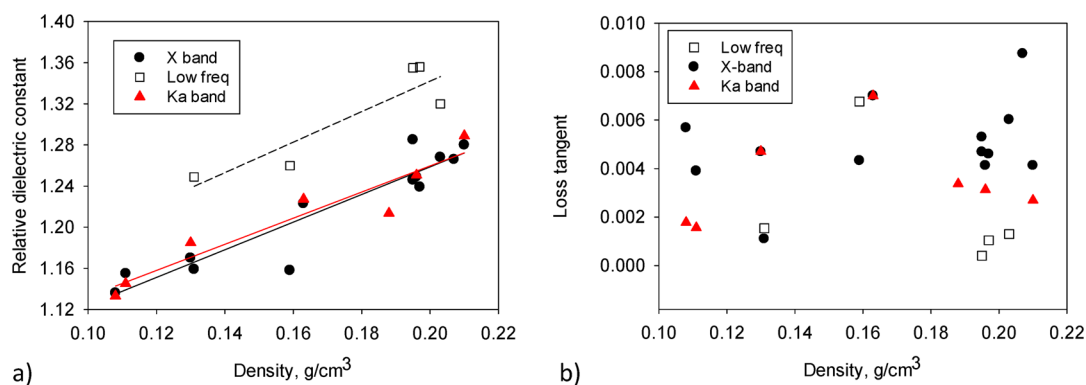


Figure 4. Graphs of (a) relative dielectric constants and (b) loss tangents of polyimide aerogels vs density.

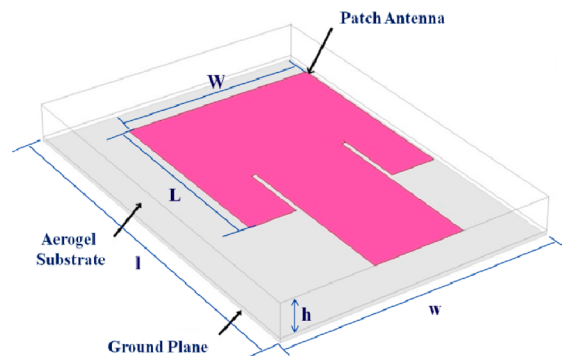


Figure 5. Schematic of printed circuit patch antenna on an aerogel substrate.

compared to BTDA, and decreases with increasing DMBZ fraction. This can be more clearly seen in Figure 3a, which shows average relative dielectric constant graphed vs DMBZ fraction for the X-band frequency range (standard error = 0.017, $R^2 = 0.93$). Mean loss tangent in the X-band also slightly but significantly decreases with increasing DMBZ fraction as seen in Figure 3b for aerogels made using BPDA (standard deviation = 0.00125, $R^2 = 0.63$). However, there is no significant

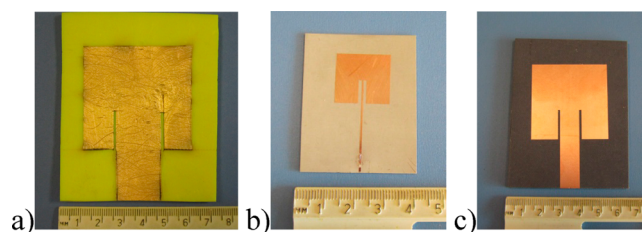


Figure 6. Photographs of patch antennas on (a) polyimide aerogel substrate fabricated using 100% DMBZ, BPDA and TAB, (b) Rogers Duroid 6010 ($\epsilon_r = 10.2$); and (c) Rogers Duroid 5880 ($\epsilon_r = 2.2$) (right).

difference in mean loss tangent with increasing DMBZ for aerogels made using BTDA over and above standard error. The difference in dielectric properties might have a contribution due to linking groups in the polymer backbone. However, the graph in Figure 4a reveals that the differences in dielectric constant seen here may be due simply to the differences in density of the aerogels. Figure 4a shows that relative dielectric constant increases linearly with density independent of the different polyimide backbone chemistry for X-band, Ka-band and low frequency ranges, similar to that observed for silica aerogels. It

Table 2. Comparison of RF and Physical Parameters of Aerogel-Based Patch Antennas and SOP Counterparts

substrate	dielectric constant	3 dB bandwidth (MHz) exp/sim	10 dB bandwidth (MHz) exp/sim	substrate dimensions $l/w/h$ (cm)	patch dimensions L/W (cm)	mass (g)
Duroid 6010	10.2	16.8/22.1	−/5.6	5.56/3.98/0.61	1.95/1.95	4.30
Duroid 5880	2.2	159/192	50.3/57.4	8.31/6.52/0.32	4.09/4.09	36.45
PI aerogel	1.16	218/255	62.1/71.2	8.82/6.88/0.41	4.80/4.80	4.18

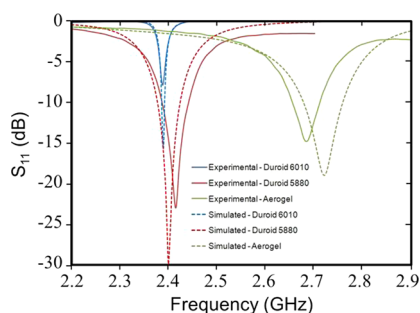


Figure 7. Plot of S_{11} vs frequency for experimental and simulated microstrip antennas fabricated from polyimide aerogel (100% DMBZ, BPDA, and TAB) and Rogers Duroid 6010 and 5880.

is not possible at this point to differentiate the effect of density on dielectric constant from the effect of backbone chemistry. However, as shown in Figure 4b, the loss tangent does not show a correlation with density. Hence, the relationship between increasing DMBZ concentration and decreasing loss tangent is related to the differing polymer backbone. It has been shown that loss tangent in silica aerogels is very sensitive to moisture content.⁶ Because aerogels made with increasing amounts of DMBZ are found to have better moisture resistance,¹³ the lower loss tangent may simply be related to lower moisture content.

On the basis of these measurements, a polyimide aerogel formulation was chosen for further study made from 100% DMBZ, BPDA, and TAB. This formulation has the lowest relative dielectric constant (1.157 ± 0.017), the lowest density and good mechanical properties. Other properties of this formulation, including surface area, porosity, mechanical properties, and morphology (as observed by scanning electron microscopy) have been previously reported.⁴ The formulation was used as a substrate for fabrication of a microstrip patch antenna and its performance compared to antennas fabricated with SOP substrates, Rogers Duroid 6010 and Rogers Duroid 5880 laminates. Microstrip patch antennas are low profile, simple to fabricate, low cost, and conformable to planar and nonplanar surfaces thereby making them suitable for aircraft and spacecraft applications where size, weight, and aerodynamic profile are major requirements.¹⁸ Rogers Duroid 5880 laminates are polytetrafluoroethylene composites reinforced with randomly oriented glass microfibers with a dielectric constant of 2.2. Rogers Duroid 6010 laminates are polytetrafluoroethylene ceramic composites with a higher dielectric constant of 10.2. The planar dimensions of a patch antenna are related to the value of the dielectric constant of the substrate.

For a given frequency and impedance matching, the lower the dielectric constant of the substrate, the larger the size of the patch antenna will be, and vice versa. Accordingly, we chose the substrates as representative of the typical trade-off in patch antenna's physical parameters (e.g., size) and relevant figure of merit (e.g., gain) influenced by the dielectric properties of the substrates.

The aerogel patch antenna was fabricated based on the schematic of the printed circuit shown in Figure 5. The patch antenna consists of a metallic circuit, in this case a gold film approximately $2 \mu\text{m}$ thick, printed via electron beam evaporation and shadow masking process on top of the dielectric substrate which in turn is coated with a film of electron-beam evaporated gold on the opposite side to form a ground plane. Specimens of the aerogel ($8.82 \text{ cm} \times 6.88 \text{ cm} \times 0.41 \text{ cm}$ in length, width, and height, respectively) were fabricated for making the patch antenna. Similar antennas were also fabricated from the commercially available Rogers Duroid 6010 and 5880. The dimensions of these antennas are given in Table 2.

Figure 6 shows the actual patch antennas fabricated using three different substrates: down-selected polyimide aerogel as well as the commercially available Rogers Duroid 6010 and 5880. The aerogel antenna was fabricated with both the antenna and ground plane deposited with e-beam evaporated gold. Note that the aerogel substrate did warp slightly on application of the gold coating. The origin of this effect and how to suppress it are currently being investigated. The patch antennas on the Rogers Duroid were fabricated using standard chemical etching procedures previously described in the Experimental Section.

The experimental performance of the antennas was determined by measuring the reflection coefficient scattering parameter (S_{11}) versus frequency using an Agilent Technologies E8361A Performance Network Analyzer (PNA) and by performing gain measurements using the substitution method according to the IEEE Standards Test Procedures for Antennas.¹⁹ Figure 7 shows plots of the experimentally measured performance of the patch antennas on all three substrates compared to simulations. Note that for all the antennas the experimental and simulated data correlate very well. It is worthwhile to highlight that the aerogel antenna exhibits both broader bandwidth and lower mass than their Duroid counterparts (see Table 2 and Figure 8). For example, the aerogel antenna has 67% higher 3-dB bandwidth than the Duroid 5880 antenna, while the mass of the aerogel antenna is nearly 1/10th that of the Duroid 5880 antenna. The Duroid

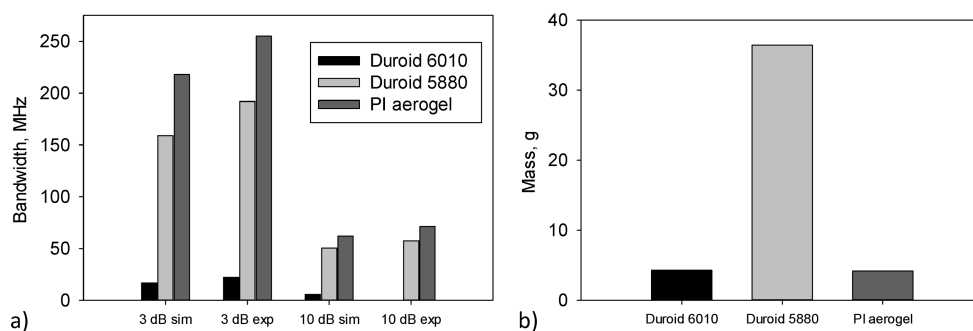


Figure 8. Comparison of (a) bandwidth (experimental and simulated), and (b) mass of antennas fabricated from polyimide aerogel (100% DMBZ, BPDA, and TAB), and Rogers Duroid 6010 and 5880.

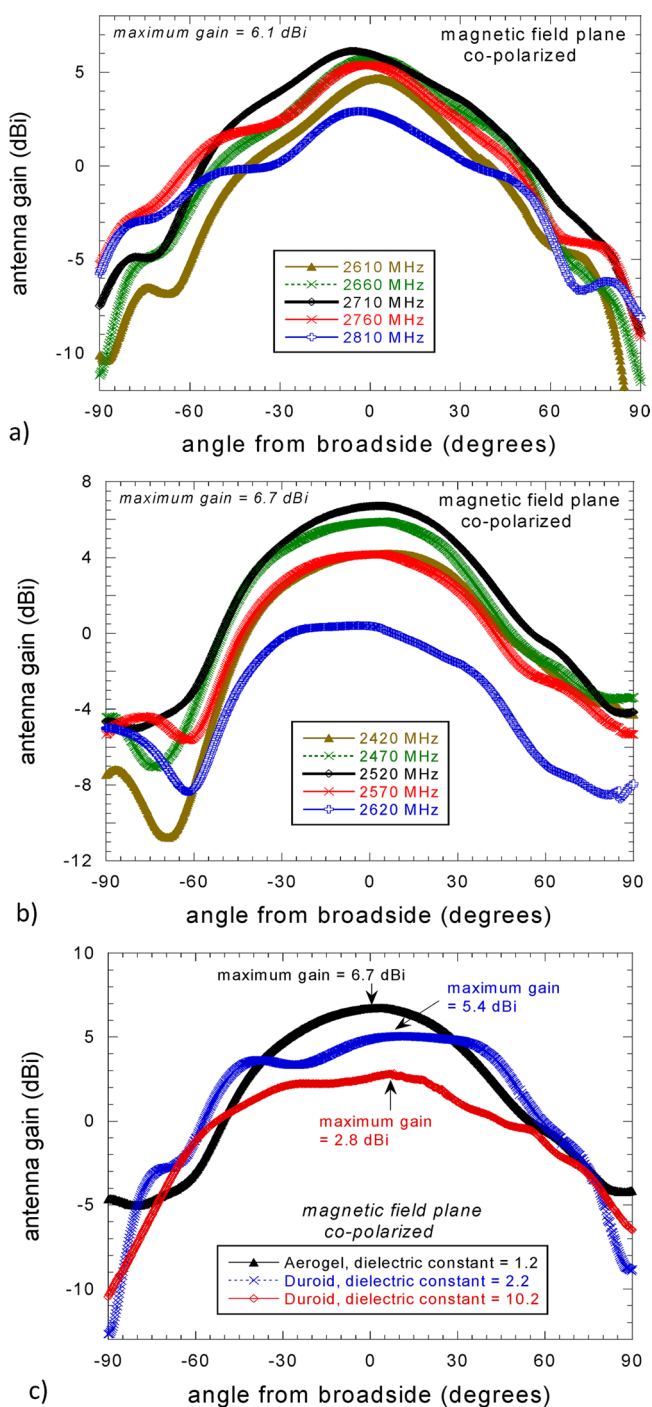


Figure 9. Antenna gain vs angle at frequencies in the 2.4 to 2.8 GHz range from broadside for (a, b) two polyimide aerogel antennas (100% DMBZ, BPDA and TAB), and (c) comparison of maximum gain for antennas fabricated from polyimide aerogel, and Rogers Duroid 6010 and 5880.

6010 antenna is comparable in mass to the aerogel antenna but the 3-dB bandwidth of the aerogel antenna is more than ten times as large. These are very encouraging results which support the potential advantages of the polyimide aerogel based antennas for aerospace applications.

Panels a and b in Figure 9 show graphs of antenna gain vs angle from broadside for two polyimide aerogel antennas, demonstrating that the results are reproducible. A comparison of the maximum antenna gain for all three antennas is shown in

Figure 9c. Note that the maximum gain is highest for the aerogel antennas. This is a significant result since this implies that when combined with the lower mass and larger bandwidth discussed above, it is feasible to develop either passive or active aerogel-based phased arrays that for a given gain could be implemented with fewer antenna elements, and at a considerably lower mass and cost, particularly for active arrays, than their current counterparts.

CONCLUSIONS

The dielectric properties and loss tangents of low-density, polyimide aerogels have been characterized at various frequencies. It was found that relative dielectric constant varied linearly with density similar to silica aerogels. However, it is not possible from this study to discern any effect of backbone chemistry on the relative dielectric constants measured from the effect of density. The loss tangent, which does not correlate with density, is affected by the polymer backbone, increasing when there are more oxygen or carbonyl bridging groups present. This effect may be related to amount of adsorbed moisture because loss tangent in silica aerogels has been shown to be moisture sensitive. The more hydrophobic aerogels made using DMBZ and BPDA have the lowest loss tangents. Relative dielectric constants as low as 1.16 were measured for polyimide aerogels made from DMBZ and BPDA cross-linked with TAB. This formulation was used as the substrate to fabricate and test prototype microstrip antennas and benchmark against state of practice commercial antenna substrates. The polyimide aerogel antennas exhibited significantly broader bandwidth, higher gain and lower mass than the antennas made using commercial substrates, hence demonstrating the feasibility of aerogel-based antennas as building blocks for high-gain, broadband, low mass phased array technology for aerospace applications.

AUTHOR INFORMATION

Corresponding Author

*E-mail: maryann.meador@nasa.gov.

Notes

The authors declare no competing financial interest.

‡Intern for NASA

ACKNOWLEDGMENTS

We thank the NASA Aeronautics Mission Directorate Seedling Fund for support of this work. We thank our NASA GRC colleagues Mr. Nicholas Varaljay and Ms. Elizabeth McQuaid for their support in the fabrication of the antennas, as well as Dr. Kevin Lambert for his support in antenna metrology.

REFERENCES

- (1) Pierre, A. C.; Pajonk, G. M. *Chem. Rev.* **2002**, *102*, 4243–4265.
- (2) Randall, J. P.; Meador, M. A. B.; Jana, S. C. *ACS Appl. Mater. Interfaces* **2011**, *3*, 613–626.
- (3) Guo, H.; Meador, M. A. B.; McCorkle, L.; Quade, D. J.; Guo, J.; Hamilton, B.; Cakmak, M.; Sprowl, G. *ACS Appl. Mater. Interfaces* **2011**, *3*, 546–552.
- (4) Meador, M. A. B.; Malow, E. J.; Silva, R.; Wright, S.; Quade, D.; Vivod, S. L.; Guo, H.; Guo, J.; Cakmak, M. *ACS Appl. Mater. Interfaces* **2012**, *4*, 536–544.
- (5) Guo, H.; Meador, M. A. B.; McCorkle, L.; Quade, D. J.; Guo, J.; Hamilton, B.; Cakmak, M. *ACS Appl. Mater. Interfaces* **2012**, DOI: 10.1021/am301347a.
- (6) Del Corso, J. A.; Cheatwood, F. M.; Bruce, W. E.; Hughes, S. J.; Calomino, A. M. *21st AIAA Aerodynamic Decelerator Systems*

Technology Conference and Seminar; Dublin, Ireland, May 23–26, 2011 ; AIAA: Reston, VA, 2011; p 2510.

(7) Hrubesh, L. W.; Keene, L. E.; Latorre, V. R. *J. Mater. Res.* **1993**, *8*, 1736–1741.

(8) Baker, S. J.; Kot, J. S.; Nikolic, N. *Proceedings of the Antennas and Propagation Society International Symposium*; IEEE Antennas and Propagation Society, June 21–26, 1998; Vol. 2, pp 1116–1119.

(9) McKenna, E. *Avionics Mag.* **2012**, *March*, 39–45.

(10) Howard, C. E. *Military Aerospace Electron.* **2011**, *22*, 26–35.

(11) Callus, P. J. DSTO-TR-1963; File number (2006/1151925)

(12) Leflour, G., Calnibalosky, C. Jaquet, H. *Proceedings from NATO RTO-AVT Symposium on Reduction of Military Vehicle Acquisition Time and Cost through Advanced Modeling and Virtual Simulation*; Paris, France, 22–25 April, 2002 ; North Atlantic Treaty Organisation: Brussels, Belgium, 2002; pp 59–1–59–10.

(13) Mochizuki, A.; Fukuoka, T.; Kanada, M.; Kinjou, N.; Yamamoto, T. *J. Photopolym. Sci. Technol.* **2002**, *15*, 159–165.

(14) Jin, Y.; Tang, J.; Hu, J.; Han, X.; Shang, Y.; Liu, H. *Colloids and SurfacesA: Physicochem. Eng. Aspects* **2011**, *392*, 178–186.

(15) Ren, Y.; Lam, D. C. C. *J. Electron. Mater.* **2008**, *37*, 955–961.

(16) Miranda, F. A.; Gordon, W. L.; Heinen, V. O.; Ebihara, B. T.; Bhasin, K. B. *NASA Technical Memorandum 102123*; National Aeronautics and Space Administration: Washington, D.C., 1989.

(17) Kittel, C. *Introduction to Solid State Physics*; John Wiley & Sons: New York, 1986; pp 370–371.

(18) Balanis, C. A. *Antenna Theory: Analysis and Design*, 2nd ed.; John Wiley & Sons: New York, 1997; pp 722–736.

(19) Procedures are described in Sections 16.1 and 12.3 of the *IEEE Standards Test Procedures for Antennas, IEEE Std. 149TM 1979* (revised 2008).